CFD EXPERIMENTS ON A LOW CRESTED SLOPING TOP CAISSON BREAKWATER. PART 2. ANALYSIS OF PLUME IMPACT

Mariano Buccino[1], Mohammad Daliri[1], Fabio Dentale[2], Mario Calabrese[1]

1. *Dept. of Civil, Architectural and Environmental Engineering, University of Napoli "Federico II". Via Claudio 21, 80125, Napoli, Italy.*
2. *Maritime Engineering Division, University of Salerno. Via Giovanni Paolo II, Fisciano (SA)*

ABSTRACT

Walkden et al. (2001) showed that severe impact events could be generated at the inner face of a sloping top caisson breakwater, as a consequence of violent wave overtopping. The authors employed the pressure impulse theory proposed by Cooker and Peregrine (1995), to develop a method capable of predicting the magnitude and distribution of loadings at the wall. It was finally recognized air trapped between the overtopping jet and the structure to have a primary role in transferring momentum to the free surface of the protected basin. Unfortunatey, that pioneering study was carried out using only 3 individual waves, with identical height and period; accordingly, no systematic analysis of this fascinating phenomenon could be provided. This paper employs results of full scale CFD experiments to fill this gap. The research outcomes, consistent with the Walkden et al. (2001) findings, suggest that the occurrence of impulsive loadings at the inner face of the breakwater is intimately correlated to the occurrence of impact pressures onto the outer wall, due to breaking waves. A physically based correction of the Walkden et al. theory has been proposed, which allows to get reasonable estimates of the pressure impulse under both quasi standing and breaking waves.

Keywords: *Numerical modeling, Computational Fluid Dynamics, Sloping top breakwater, wave force, wave impact.*

1. INTRODUCTION

In 2001, Walkden et al. published the results of laboratory experiments carried out on a small scale model of a sloping top caisson breakwater. Using short test runs, the authors generated 3 non breaking individual waves, with a height of 0.17 m and a period of 1s. The waves were shown to violently overtop the breakwater crest, producing a remarkable impact onto the inner face of the breakwater. Walkden et al. used the impulse approach concept originally introduced by Cooker and Peregrine (1995), to develop a theory, which allowed the prediction of the pressure impulse distribution along the rear wall. They also argued air to play a significant role in the phenomenon, since the cushion trapped between the overtopping jet and the structure was able to transfer a certain amount of momentum to the free surface in the protected area. The occurrence of impact loadings as a consequence of an overtopping event, is of course of great interest to engineers, because even if such loadings are likely irrelevant to the breakwater stability, they can cause local breakage of either the caisson or the superstructure. The need of an adequate degree of knowledge about this topic is nowadays further increased by the long term rise of the mean sea level, which makes the overtopping events increasingly frequent.

Yet, surprisingly enough, no research study has followed the Walkden et al. work. Accordingly, a significant uncertainty exists on a number of items, such as:

- ✓ what is the mechanism by which wave overtopping can generate impact events;

- ✓ what is the magnitude of loadings (peak pressure, maximum force etc) in response to different wave parameters;
- ✓ what is the degree of predictability of the phenomenon (either in a deterministic or probabilistic sense);
- ✓ what is the influence of the model scale on the Walkden et al. measurements;
- ✓ what is the degree of reliability of the Walkden et al. theory.
- ✓

This paper employs the full scale CFD experiments described in Buccino et al. (2019) to start filling those gaps.

After a qualitative description of the mechanisms that govern impacts occurrence (Section 2), a quantitative analysis is provided in the Subsection 3.2. Then, predictability is studied in the frame of a probabilistic approach (Subsection 3.3). After analyzing the pressure distribution characteristics, with a special focus on the role of air entrainment (Subsection 3.4), a comparison with the Walkden et al. theory is carried out in Subsection 3.5.

Throughout the paper, results of numerical experiments are compared to those of the Walkden et al. physical model tests.

2. IMPACT EVENTS INDUCED BY WAVE OVERTOPPING

Fig. 1 compares different stages of an overtopping event, as observed in the CFD flume (test 2B) and as presented in the Fig. 5 of the Walkden et al. (2001) paper.
The picture shows a good consistency, although the breakwater crown geometries are slightly different from each other; this because the structure used in the numerical tests was initially thought to model a sloping face Wave Energy Converter (Vicinanza et al., 2015; Buccino et al., 2016) superimposed to a conventional vertical-face breakwater. Details of the interaction between overtopping jet and protected basin are displayed in Fig. 2.

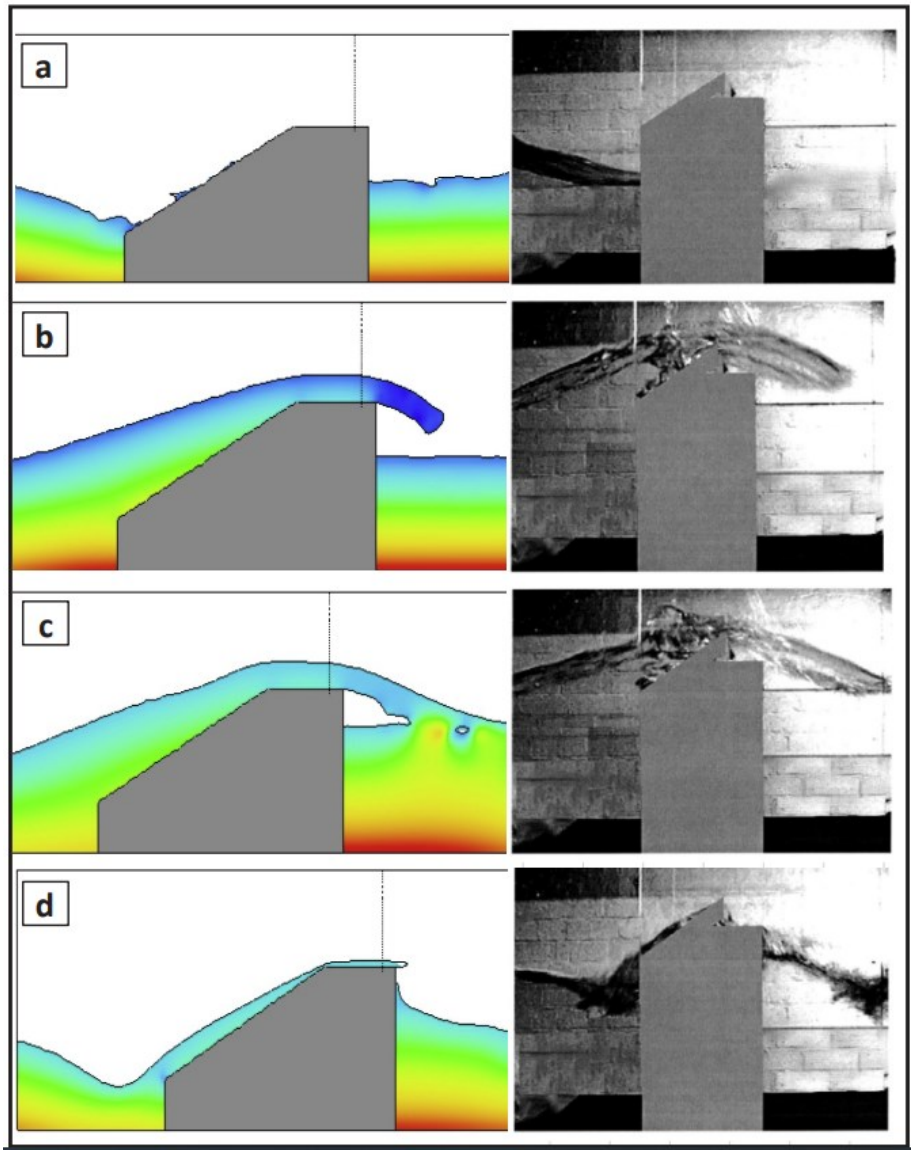

Figure 1. Different phases of an overtopping event as observed in test 2B and in Walkden et al. (2001). a) wave trough at the wall; b) jet passes over the superstructure causing a high landward load; c) The jet plunges into the harbor; d) water level rises at the rear face and lowers at the front

Firstly, a jet of water with a large momentum hits the harbor, here inducing significant inertia forces (Fig. 2a). Hence, the water between the jet and the wall is pushed upwards, giving rise to a fast up-rush motion (Fig. 2b). At the same time, a very steep wave front is generated in the neighborhood of the falling point of the jet (Fig. 2c), which collapses down (Fig. 2d) creating a secondary crest that moves towards the wall. From the process just described, two different impact events may arise.

One occurs because pressures at the wall counteract the huge inertia transferred to the water by the overtopping jet; according to Walkden et.al (2001), we will refer to this event as “plume impact”.

The other is related to the secondary crest; if it arrives at the wall when the water level is in phase of down rush (Figure 3.a), then the water surface considerably steepens and a plunging-like impact takes place (Figure 3.b), which we term “secondary plunging impact”. Otherwise, if the crest approaches the wall during the up rush phase (Figure 4), the motion will solve in a simple vertical oscillation.

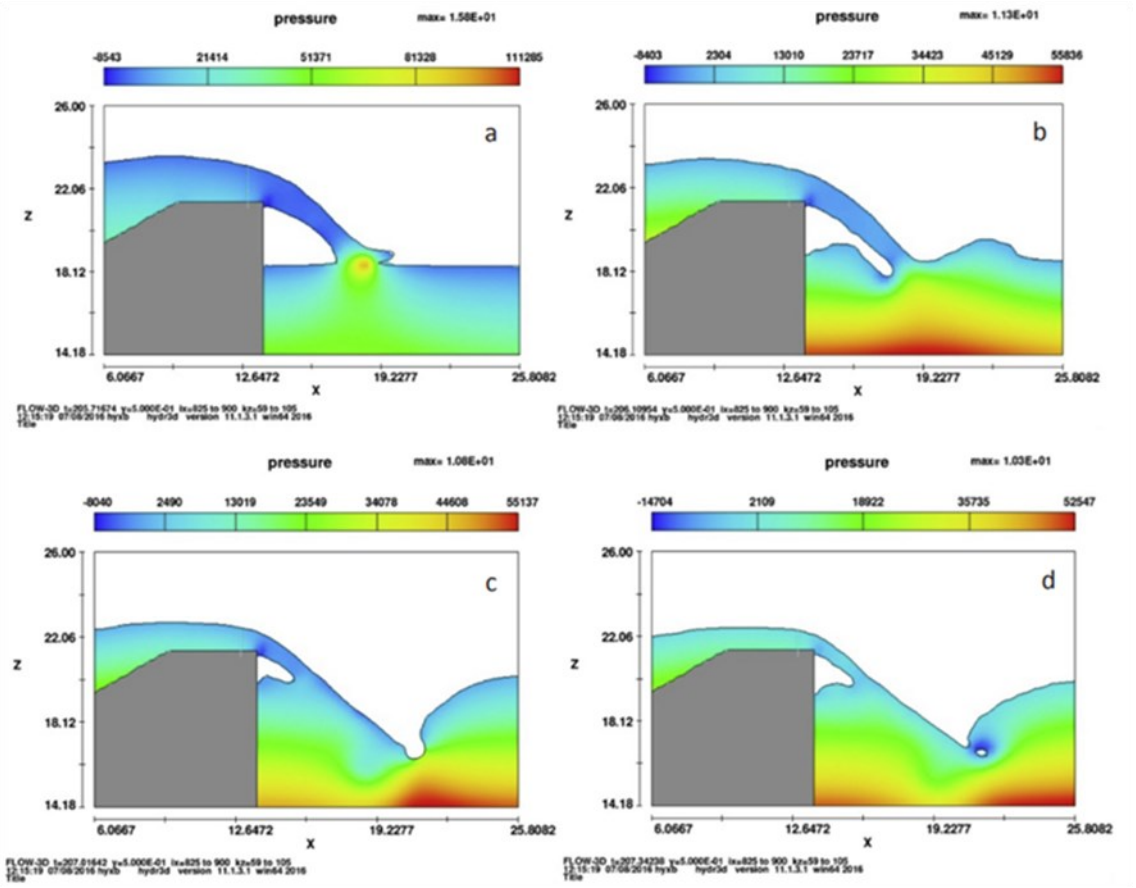

Figure 2. Example of secondary plunging impact

Altogether, characteristics of the “secondary plungings” do not differ a big deal from those widely studied in the past for conventional vertical face breakwaters. For this reason, the rest of this paper will focus on the “plume impact” only.

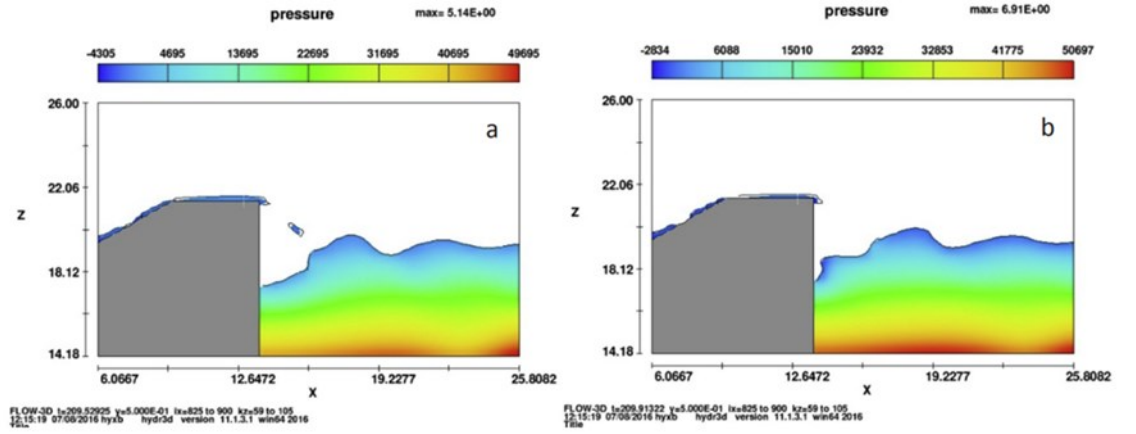

Figure 3. Example of secondary plunging impact.

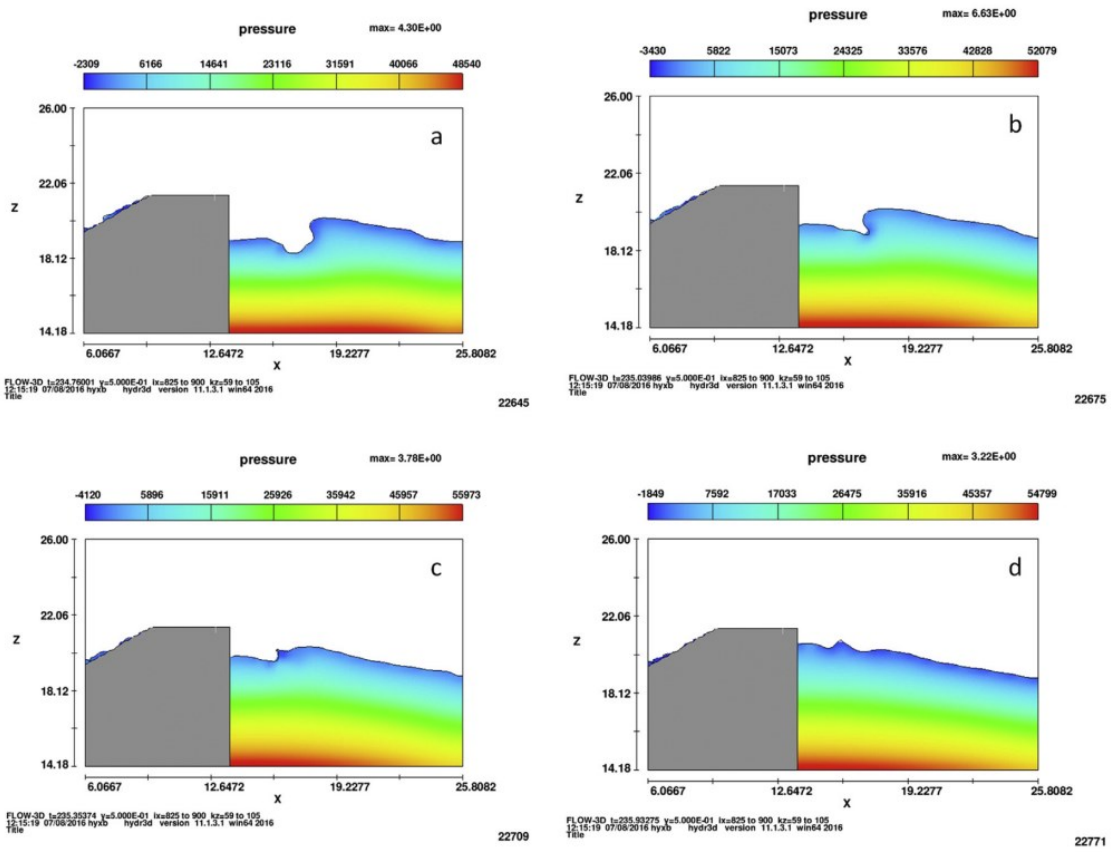

Figure 4. Secondary crest approaching the wall during up rush (no secondary plunging is created).

Notwithstanding, as a starting point for future research works, the Table 1 reports the maximum and average values of the force exerted by secondary plungings onto the inner face of the breakwater; it is seen wave forces can attain remarkable magnitudes, overcoming 40% of the hydrostatic thrust 0.5ρgd2. The last column of Table 1 finally displays the percentage of observed impacts, which always exceeds 50%.

Table 1
Summary of secondary plunging characteristics.

Test code	$F_{max}/\rho gd^2$	$F_{ave}/\rho gd^2$	percentage of secondary plunging events
1A	0.107	0.037	54
1B	0.046	0.026	64
1C	0.0459	0.022	51
2A	0.177	0.091	79
2B	0.228	0.090	85
2C	0.108	0.047	90
N1	0.404	0.124	88
N2	0.385	0.130	70
3A	0.243	0.164	67
3B	0.277	0.143	87
4A	0.191	0.128	70

3.1 ANALYSIS OF PLUME IMPACT

3.1 Loading characteristics

Macrocharacteristics of “plume impacts” as observed in the CFD experiments, are generally similar to those described by Walkden et.al (2001); an example is shown in Figure 5, where one of the events recorded during the test 1A is compared to the Figure 7 of the Walkden et al. paper. In the

graph, the time history of the horizontal force exerted on the breakwater (including both front face and rear face pressures) is standardized (subtracting mean and dividing by standard deviation) and plotted against the time to period ratio, t/Tp.

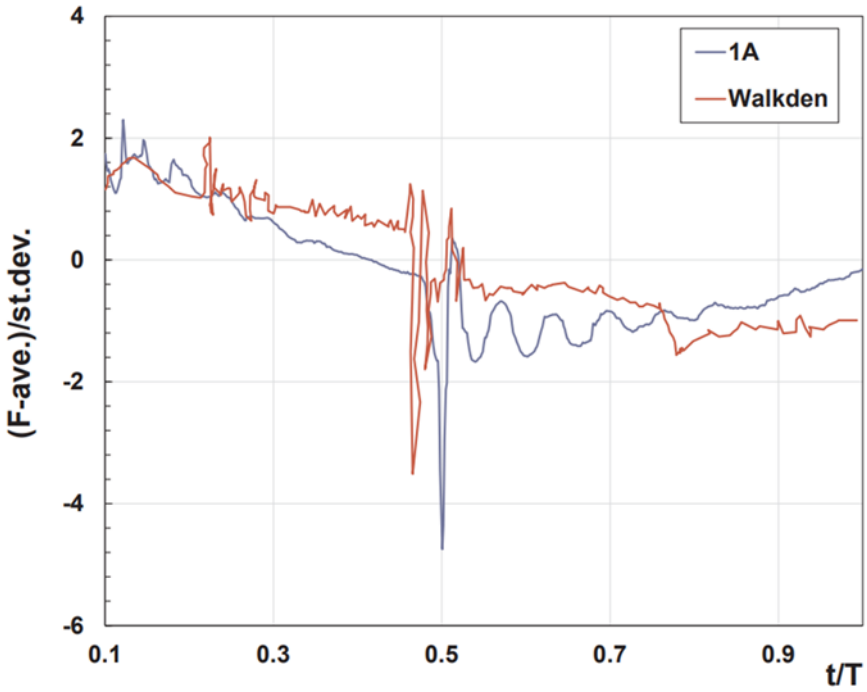

Figure 5. Comparison between a plume impact recorded in the test 1A and Figure 7 of Walkden et al. paper.

Despite the shape of the loading waves seems to be slightly different, the phases in which the impacts occur are consistent to each other (around 0.5 T) and so is the magnitude of the (standardized) peaks.

The details of the “numerical” impact event are shown in Figure 6. The peak of force, Fmax, occurs 0.15s after the overtopping jet has touched the rear basin (upper panel). The distribution of pressure at the instant of Fmax (lower panel) has a peak located well below the still water level; unlike Walkden et although, Fmax takes place as pressures on the front face are negative, i.e. when the water level at the outer wall is down-rushing.

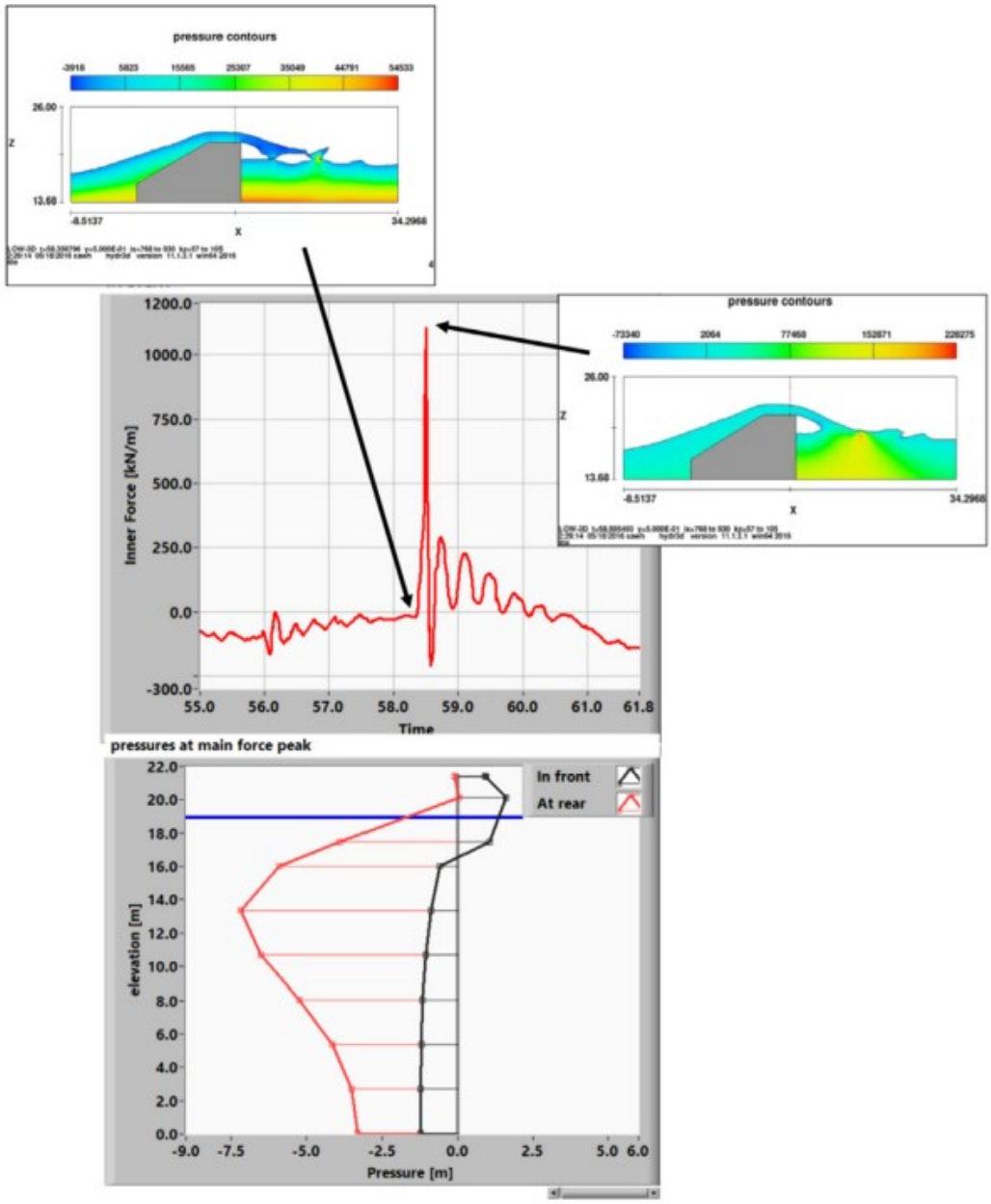

Figure 6. Details of a plume impact (test 1A). Negative pressures are directed seawards

3.2. Quantitative analysis

To give a quantitative description of the phenomenon under study, four non dimensional engineering variables have been selected and namely (Figure 6):

1. The force peak F′,

$$F' = F_{max}/(\rho q_{max}\sqrt{2gR_c}) \quad (1)$$

in which qmax is the maximum of the overtopping rate in a wave cycle, Rc is the crest freeboard and 2gRc is the ballistic fall velocity. In this way the plume impact intensity is directly related to the magnitude of the overtopping process.

2. The rise time t', given by the ratio between the rise time of Fmax (tr) and the peak period;
3. The force impulse IF′, defined as:

$$I'_F = I_F / A_I \tag{2}$$

in which IF is the impulse of the plume impact (Fig. 7) and AI is the average impulse per cycle of the wave force acting onto the breakwater's outer face. AI is calculated as follows:

$$A_I = \frac{1}{N_w} \int_{t_s}^{t_f} F_{out}\, dt \tag{3}$$

in which Nw is the number of waves, Fout is the force acting on the outer wall, and ts and tf are the starting and the final instants of the test respectively.

4. The non-dimensional maximum pressure at the peak of force p' = pmax/ρgHm0

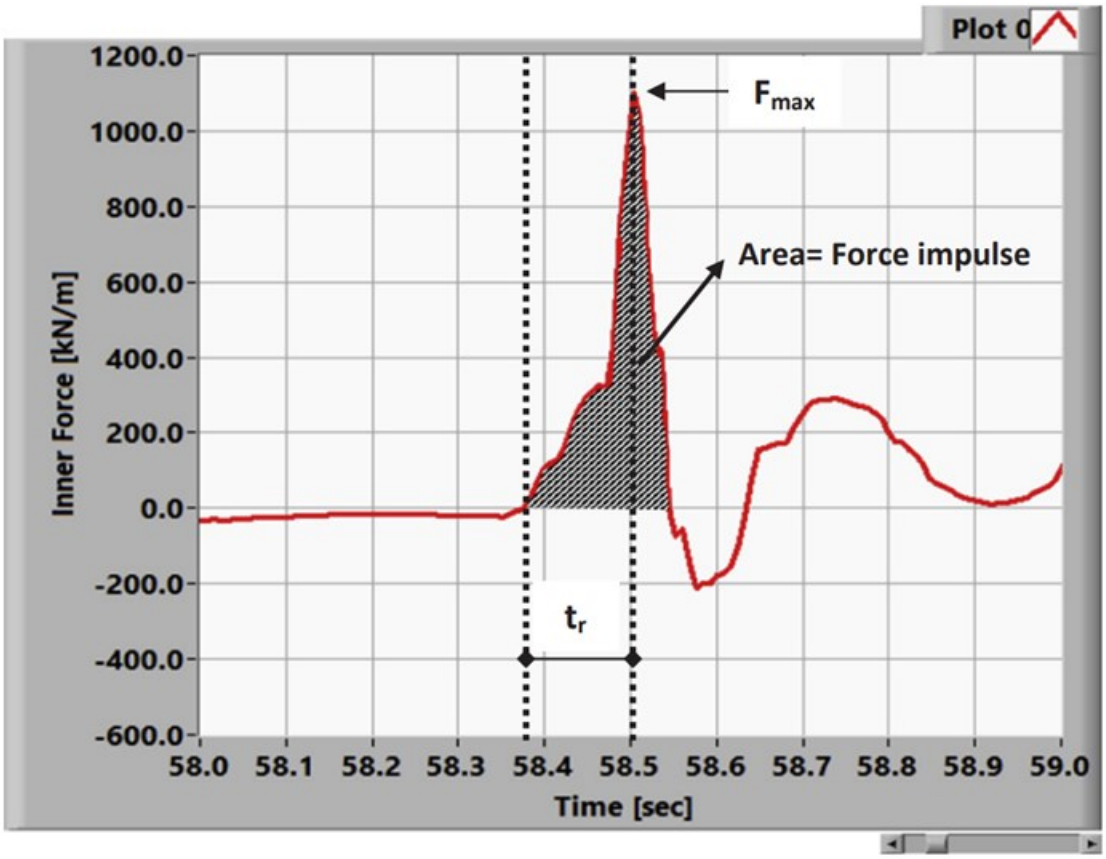

Figure 7. Definition sketch for the non dimensional engineering variables

Table 2 reports the minimum and maximum values observed through the 11 tests here presented.

Table 2. Minimum and maximum values of non dimensional engineering variables

	MIN	MAX
F'	0.157	8.998
t'	0.001	0.056
I_F'	0.001	0.516
p'	0.046	1.462

Each quantity is seen to span over 1 or 2 orders of magnitude, highlighting that plume impact is affected by a large variability, like all the impact phenomena. For example, the force impulse I'F can be either very small or of the same order as the impulse transferred by the waves to the outer face of the breakwater.

Same holds for pressure; regarding this variable it is also worth to mention that the maximum value measured in the CFD experiments (p' = 1.46) is very close to that observed by Walkden et al. in their experiments, i.e. 1.37. This suggests that plume impacts generate loadings far less intense than those exerted by violent plunging breakers on the front face of vertical breakwaters (p'>10).

3.3. Predictability

The high variability observed, suggests that characteristics of plume impacts can be predicted only in the frame of a probabilistic approach. Consistently, each of the quantities introduced above, has been modeled as a random variable, X, with a probability density function in the form:

$$pdf = f(X;\theta) \tag{4}$$

where θgenerically denotes a group of parameters related to the pdf moments (mean, variance, etc.). In practice, for each test all the non dimensional variables (peak of force, rise time, impulse and

maximum pressure) have been measured wave by wave, so obtaining a sample for the Eq.(3). Thus, predictability is studied here by:

1. researching the most appropriate shape of the pdf ;
2. analyzing the relationships between θ, or equivalently the pdf moments, and the bulk descriptors of the incoming sea states, such as wave steepness Hm0/L0p, relative crest freeboard Rc/Hm0 etc.

As for the mathematical form of the pdf, the lognormal distribution resulted the most suited for all quantities (e.g. Figure 8); this agrees with many previous studies on impact loadings, such as those by Kirkgoz (1995), Vicinanza (1997), Calabrese et al (2000) and Buccino et al (2015).

As widely known, the lognormal pdf depends on two parameters and namely the scale factor μL and the shape factor σL; they can be easily related to the mean and variance of X, using the formulae:

$$E(X) = \exp[\mu_L + \frac{1}{2}\sigma_L^2] \tag{5}$$

$$VAR(X) = \exp[2(\mu_L + \sigma_L^2)] - \exp(2\mu_L + \sigma_L^2) \tag{6}$$

In predicting E(X) and VAR (X) only F′, t' and p' are considered, because the impulse can be can be easily estimated by multiplying force peak and rise time.

As shown in the Figs. 9 and 10, the mean of F′ and p' can be predicted relatively well as function of the fictional wave steepness:

$$s_{0p} = 2\pi \cdot \frac{H_{m0}}{gT_p^2} \tag{7}$$

and the crest parameter:

$$R_p^* = \frac{R_c}{H_{m0}} \cdot \sqrt{\frac{S_{op}}{2}} \tag{8}$$

which has been originally introduced by Owen (1980) as a predictor of the overtopping rate. The following curves have been obtained:

$$E(F') = 104.94 \cdot (R_p^*)^{1.18} \; R^2 = 0.85 \tag{9}$$

$$E(p') = 0.88 \cdot s_{0p}^{0.4} \; R^2 = 0.77 \tag{10}$$

whereas only a weak dependence of rise time on wave steepness has been found:

$$E(t') = 0.052 \cdot s_{0p}^{0.4} \; R^2 = 0.39 \tag{11}$$

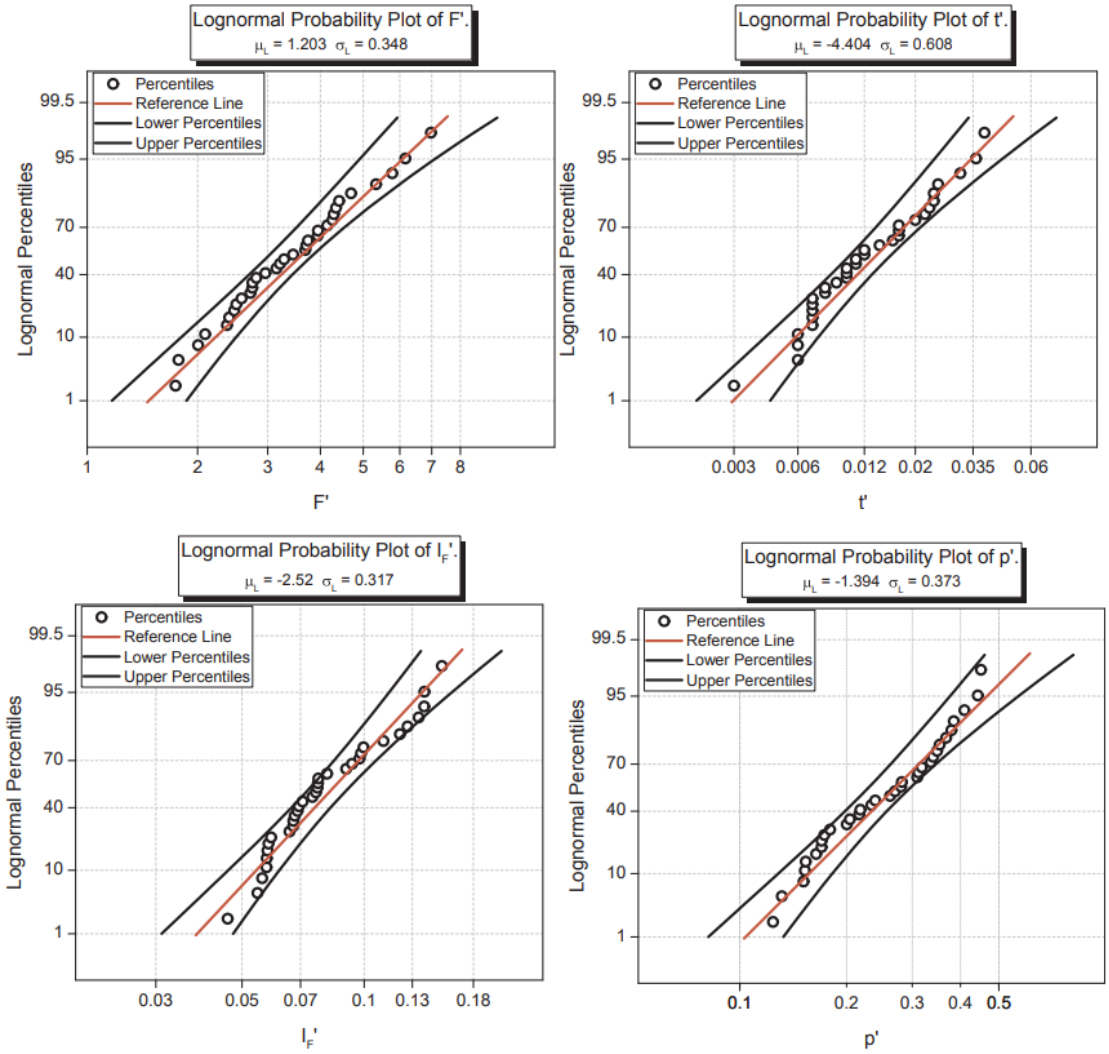

Figure 8. Example of non dimensional variables plotted on a log-normal chart (Test 3A)

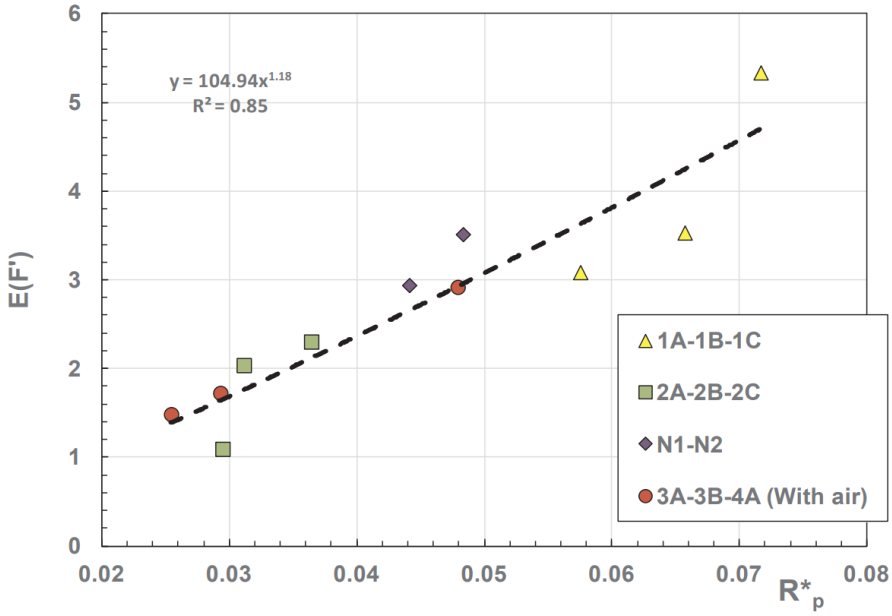

Figure 9. Mean of the non dimensional force peak, as function of the crest parameter.

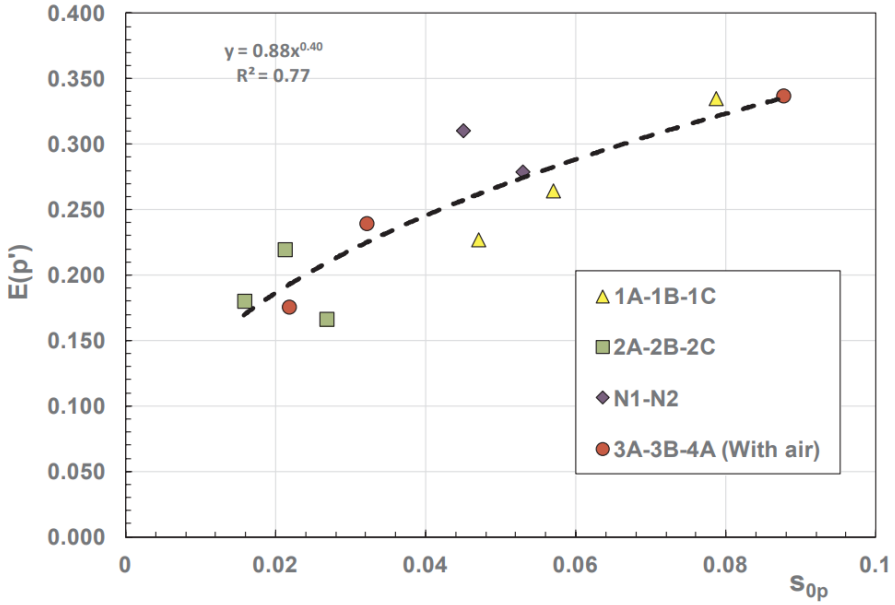

Figure 10. Average non dimensional pressure as function of wave steepness

Previous results (particularly Eqs. (9) and (10)) appears rather interesting, especially if one takes into account that sop and Rp ∗ have been found to rule the occurrence of impact events onto the outer face of the structure (Buccino et al., 2019). Basically, the equations above suggest that the risk of violent plume impacts is significantly correlated to the risk of impact loadings onto the front face of the structure; this because the high velocities associated with wave breaking augment the momentum of the overtopping flow, which is finally converted into inertia forces in the protected area. As far as variance is concerned, no clear trends were observed.
An example is given in Fig. 11, where the standard deviation of p' is plotted against s0p. It is likely this behavior to be the result of sampling effects related to the small number of waves included in each test; it is clear that while few data might be enough to have a stable estimate of the first order moment of a distribution (i.e. the mean), this is not the case for the second order moment, which is inherently more affected by the extreme values in a sample. In lack of clear relationships, the standard deviations obtained from each test have been averaged and reported

in Table 3, as a reference for future research works.

Table 3
Mean values of standard deviations for non dimensional engineering variables.

Quantity	mean value obtained from all the tests
F′	1.24
t’	0.0072
p’	0.135

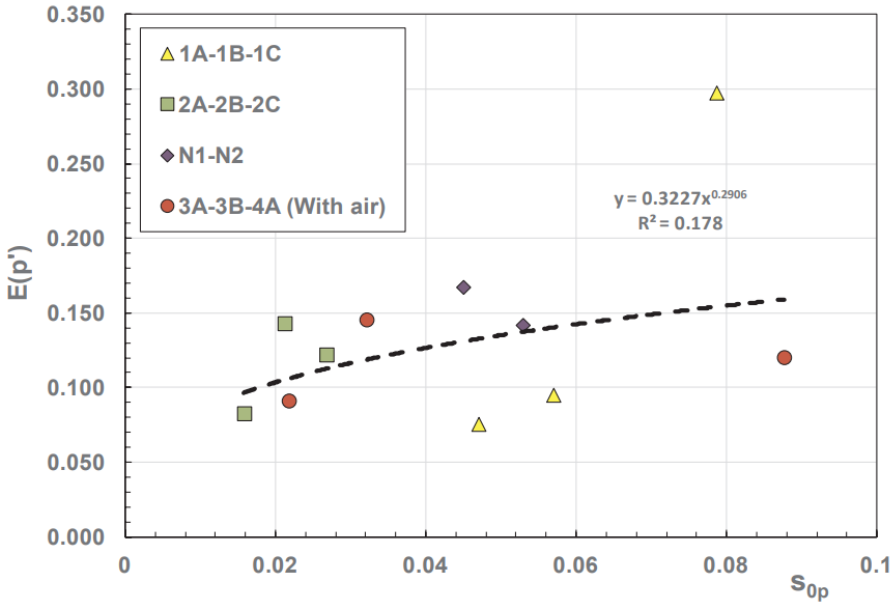

Figure 11. Standard deviation of non dimensional maximum pressure as a function of wave steepness.

3.4. Pressure distribution characteristics

So far, the inclusion of air in the simulations has never produced a significant effect on test outcomings; in the Figures from 8 to 10, data of the experiments conducted with a biphase fluid lie in the same cloud as tests run without air. Similar results have been found in Buccino et al. (2019) with respect to the quasi-static part of wave loadings. Oppositely, a clear influence on the pressure distribution at the peak of plume impact has been detected. Fig. 12 plots the position of the pressure barycenter from the still water level, ZG, versus s0p. ZG is averaged event by event within each test and made non dimensional by the still water depth d. It is seen experiments with air to have a center of mass closer to the still water level; on the other hand for the tests with a single fluid ZG ≈ 0.5d, indicating an almost uniform distribution. The difference above described is even more evident if the position of the maximum pressure, Zmax, is considered. In Fig. 13, data with air exhibit a maximum very close to the still water level, whereas for the mono-phase fluid, the peak of pressure is located between 0.1 and 0.5 d. Moreover, a clear trend with relative crest freeboard is observed. As shown in the next Section, the above findings are well consistent with those of Walkden et al. in comparing their theoretical approach for pressure impulse to experimental measurements, the authors noticed that neglecting of air contribution led to a theoretical distribution of loadings just more uniform, and with the maximum located lower (see Fig. 13 of the Walkden et al. paper).

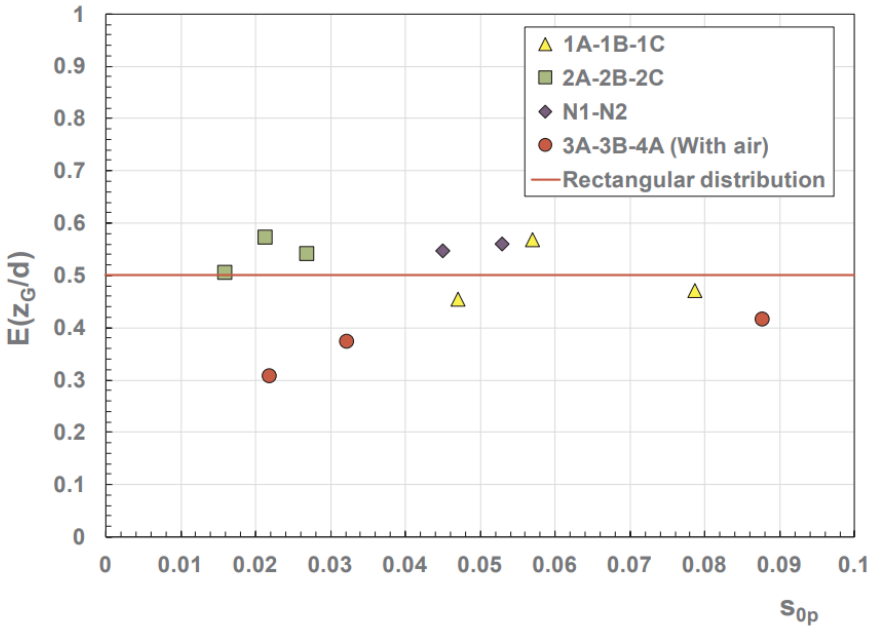

Figure 12. Average position of pressure barycentre as function of wave steepness.

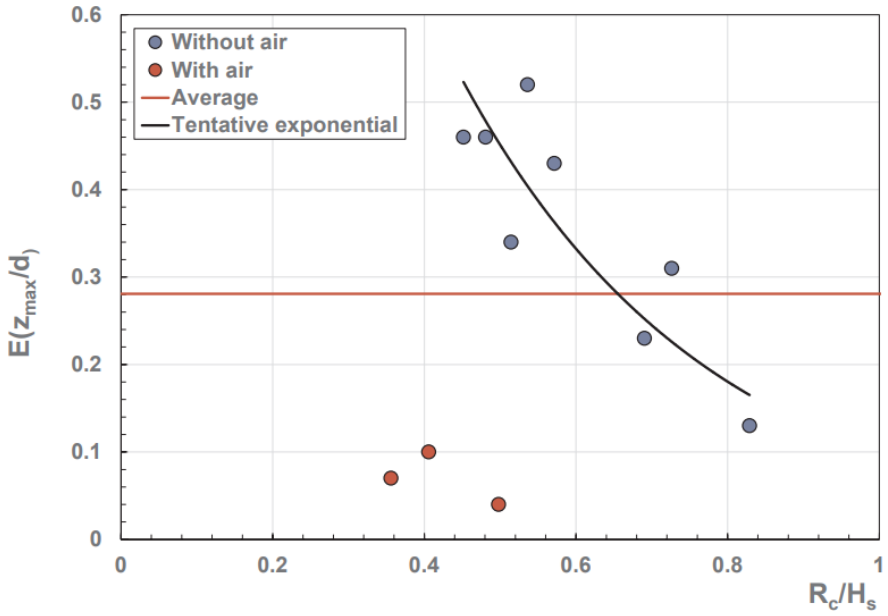

Figure 13. Average position of the pressure peak as a function of the relative crest freeboard

3.5. Analysis of pressure impulse

3.5.1. General characteristics

Fig. 14 shows some examples of pressure impulse distributions for tests 1A (mono phase fluid, left panel) and 4A (biphase fluid, right panel). On the ordinates, the vertical distance from the sea bottom (d-z) is made non dimensional by the water depth d; on the abscissas, the pressure impulse (Pimp) is divided by its maximum value along the wall (Pimp, max). Filled circles refer to the Walkden et al. measurements, which, as anticipated, are seen to be well consistent with CFD simulations only if the effect of air is accounted (i.e. test 4A). This supports the argument that air significantly influences distribution of loadings.

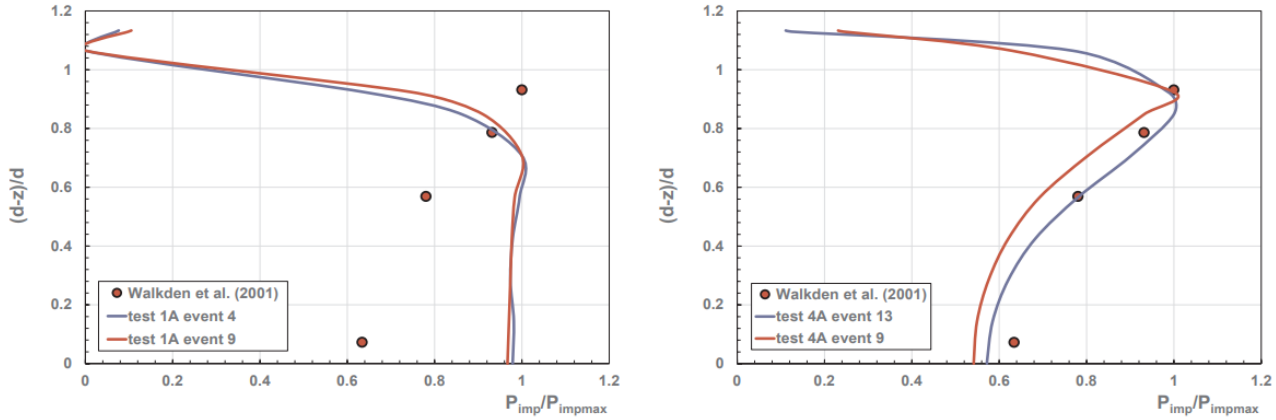

Figure 14. CFD pressure impulse events vs. Walkden et al. (2001) experiments. Left panel: test 1A (monophase fluid). Right panel: test 4A (biphase fluid).

3.5.2. Pressure impulse prediction

Walkden et al. (2001) developed a very interesting theoretical model to predict the distribution of pressure impulse associated with a plume impact event. The model starts from the "impulse approach", originally introduced by Cooker and Peregrine (1995), in which impact events are studied by retaining only pressure and inertia terms in the Navier-Stokes equations. This leads pressure impulse to be governed by the Laplace Equation:

$$\nabla^2 P_{imp} = 0 \tag{12}$$

Walkden et al. basically solved two boundary problems; in the first (Fig. 15), the overtopping jet is treated like a rectangular solid (width a, height b), which falls at the ballistic velocity V = 2gRc . The solution gives the pressure impulse at the base of the falling block, Pov, which is then used as a boundary condition in the second differential problem (Fig. 16); the latter furnishes the distribution of Pimp at the wall. Walkden et al. compared their method against three individual waves only; they argued that for theoretical predictions to compare well with measurements, the effect of the air pocket enclosed between the overtopping jet and the wall (Fig. 16) had to be properly modeled. In fact they assumed the air pocket to transfer to the water surface a pressure impulse equal to the 80% of Pov. Obviously, in this paper the effect of air pocket is accounted only for tests conducted with air. In the other cases, the pressure impulse beneath the falling jet has been set equal to zero. Some examples of the obtained results are pictured in Fig. 17. In spite the general trend of Pimp is captured, significant under predictions have been detected. A more general view of the model performances can be obtained by examining the root mean square error RE, defined as:

$$RE = E_{ev.}\left[\sqrt{E_{wall}(P_{meas.} - P_{calc.})^2}\right] \tag{13}$$

in which the subscripts ''meas'' and ''calc'' stand for measured and calculated respectively, Ewall indicates averaging along the wall and Eev indicates averaging through the events of a given test. The Fig. 18 shows that with the exception of the test 3A, the Walkden et al. approach provides good estimates when quasi-standing waves take place in front of the structure; on the other hand, the quality of predictions reduces in presence of breaking or broken waves. A simple explanation of this behavior is that when waves break, high flow velocities develop and the overtopping current on the structure top possesses a remarkable kinetic height, which is ignored by the method. A way to simply include this effect in the first boundary problem is applying the complete Bernoulli theorem:

$$\frac{U^2}{2g} + R_c = \frac{V^2}{2g} \tag{14}$$

where V is the fall velocity and U is the speed of the overtopping current. Thus we have

$$V = \sqrt{2gR_c + U^2} \tag{15}$$

which clearly reduces to the Walkden et al. hypothesis as U → 0 . The following general formula has been chosen to model U:

$$U = F_r \cdot \sqrt{gh_0} \tag{16}$$

where h0 is the height of the overtopping current just before the inner edge of the breakwater top (Fig. 19), at the instant of the plume impact. The Froude number Fr is expected to be of the order of 1 for quasi standing tests, since the overtopping process is there relatively slow and accordingly the current on the horizontal crest can be considered approximately in critical conditions; on contrary, in presence of breaking or broken waves, it may considerably increase.

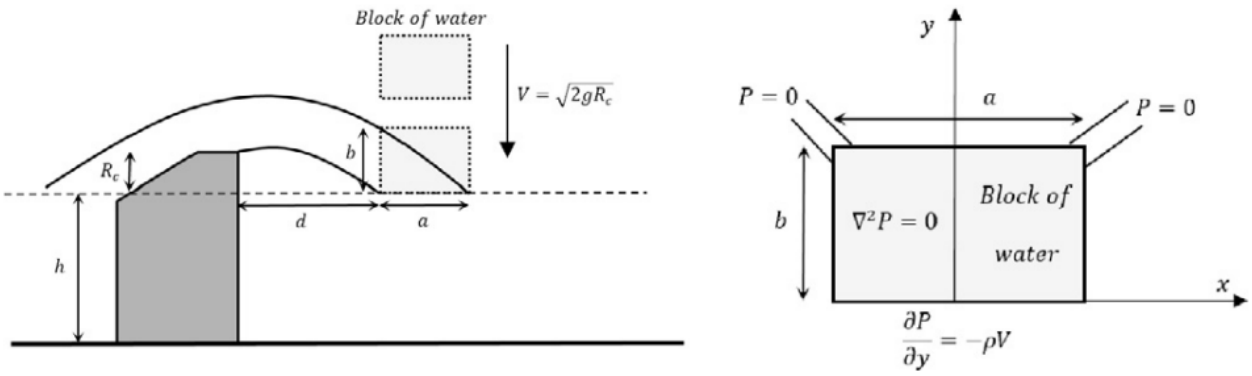

Figure 15. First boundary problem in the Walkden et al. (2001) method.

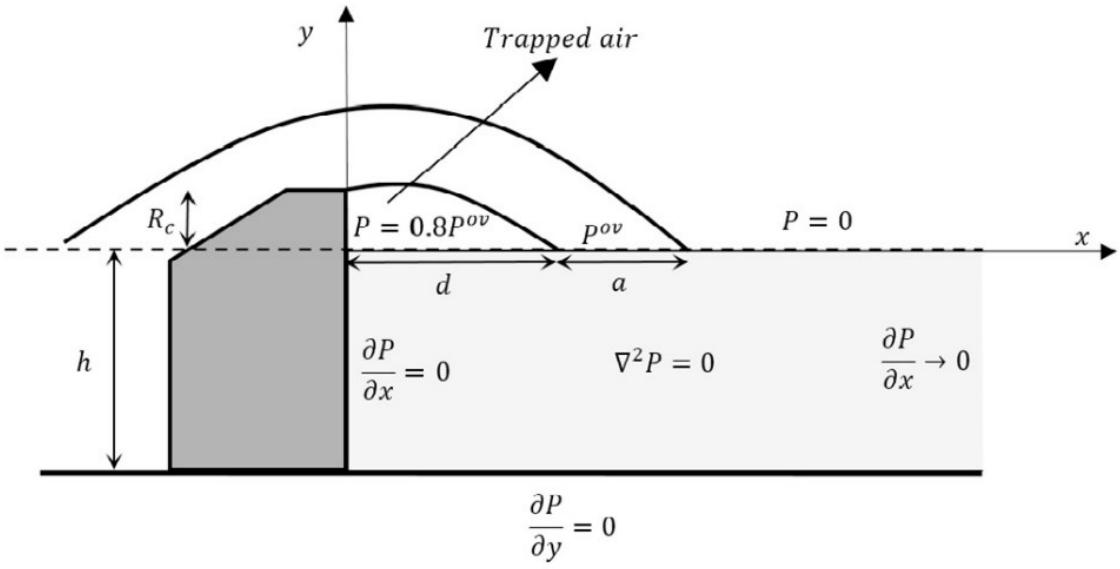

Figure 16. Second boundary problem of the Walkden et al. method.

Despite Fr should vary, in principle, event by event, a single value has been calculated for each test, by minimizing RE. The Fig. 20 compares the values of the root mean square error with and

without the correction of Eq. (15). The graph shows only small reductions of RE for quasi-standing waves, suggesting that the kinetic height of the overtopping current is negligible for these cases, consistently with the Walkden et al. findings. On contrary, for breaking waves the Eq. (15) produces significant improvements of the predictions, as pictured in Fig. 21 for the events of Fig. 17. As shown in Fig. 22, the optimal Froude number is well predictable in function of the crest parameter R*p, with a trend which is independent of the inclusion of air in the simulation. A supplementary analysis has been carried out to assess the effect of varying the pressure impulse transferred by the air pocket. In Fig. 23, the latter is expressed in terms of percentage of Pov (Fig. 16), whereas the Froude number has been calculated using the exponential form of Fig. 22. It is seen, the percentage associated to the minimum RMSE equals 50% for test 4A, 70% for test 3A and 80% for test 3B. This range is physically reasonable and consistent with the expectations by Walkden et al. (2001). On the other hand, the weight of the air pocket on the general performance of the predictive method appears uncertain, as only in one case (test 4A) an appropriate selection of the percentage of Pov leads to a significant reduction of RE.

3.6 A discussion on the role of air compressibility

Eight tests out the 11 here discussed have been carried out with a monophase fluid, whereas in the remaining 3 cases air has been treated as incompressible. From a fluid-dynamic point of view, the latter choice is justified by the fact that velocities associated with the overtopping process are o (2gRc), that is about 7 m/s for the breakwater here employed. Under this situation, a Mach number larger than 0.3 is obtained for a sound speed less than approximately 23 m/s; according to the well known Hsieh and Plesset (1961) formula, such a low value could be achieved for a volume fraction of air in water larger than 50%, which is of course extremely high. Even in lack of direct measurements for the case of an overtopping jet, it could be of interest to mention that during the analysis of field data on violent impacts at Alderney breakwater, Bullock et al. (2000) observed an aeration rate in the range 5%–15%, corresponding to sound speeds varying between 45 and 85 m/s. The results presented in the previous sections essentially confirm the Walkden et al. (2001) findings, either about the occurrence itself of violent impact events at the rear wall, or with respect to the role of the air pocket trapped between the inner face of the structure and the overtopping jet. Regarding the latter, it is worth highlighting that its role in the “plume impact” basically consists in transferring a part of the pressure impulse to the water surface. This is inherently different from the case of “direct impacts” occurring at the front face of the break waters, where the air pocket is known to cushion the impact of part of the water mass, producing an increase of the duration of the peak pressure, diminishing, at the same time, its magnitude (Bullock et al., 2001). It is also noteworthy that just this behavior poses significant problems in scaling results of laboratory experiments (Kortenhaus and Oumeraci, 1999; Cuomo et al., 2010), also considering the different survivability time of air bubbles between fresh and salt water (Peregrine, 2003). In this study, even if modeled as incompressible, that is assuming an infinite natural oscillation frequency, the air pocket has been found to transfer to the water surface an amount of loading perfectly consistent with the Walkden et al. findings.
This is generally in line with the conclusions of a recent research study carried out by Gaeta and Lamberti (2015) using the CFD code COBRAS2. In analyzing the impact of water waves on a horizontal deck, the authors found both the compressible and incompressible bi-phase solvers to give good predictions of laboratory experiments, with little differences between each other. Gaeta and Lamberti also noticed that the use of a compressible bi-phase solver significantly increases the computation times. However, it is clear that a certain part of the “plume impact” physics couldn't be modeled in this study; this includes the propagation of the impulsive peaks, the natural oscillations of

the air pocket, clearly visible in the Walkden et al. experiments, or the possible occurrence of “bounce back” phenomena. as described in Wood et al. (2000). These items will be discussed in a future investigation with the aid of appropriate research tools.

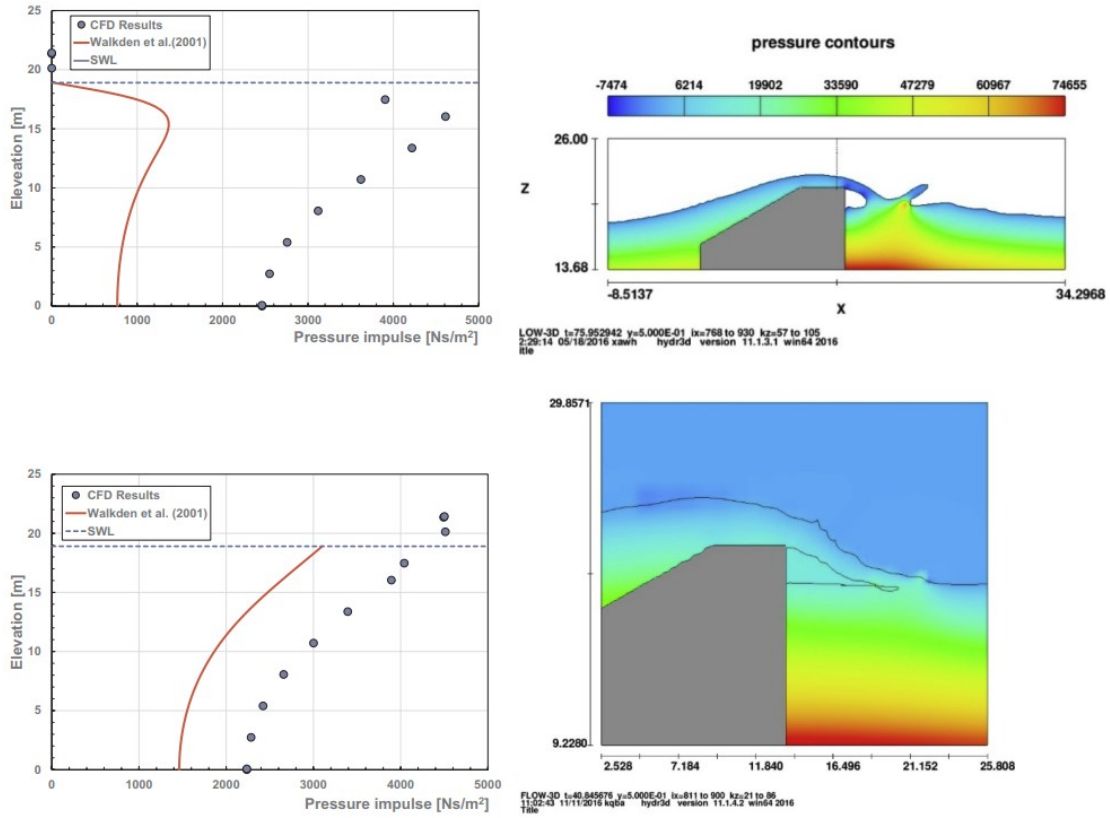

Figure 17. Examples of measured pressure impulse distribution. Upper Panel: Test 1A (no air); Lower panel: Test 4A (air entrainment is simulated).

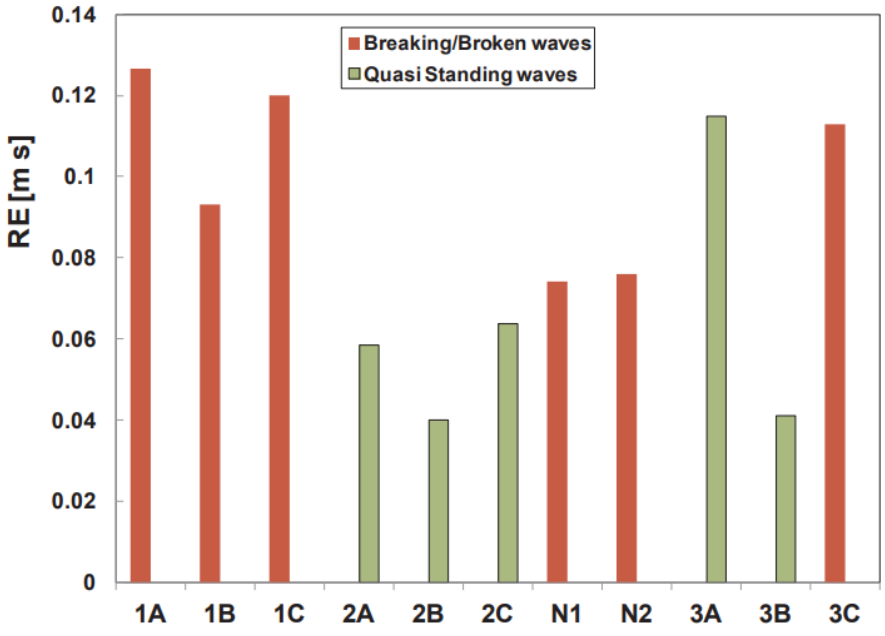

Figure 18. Root mean square error for the Walkden et al. method.

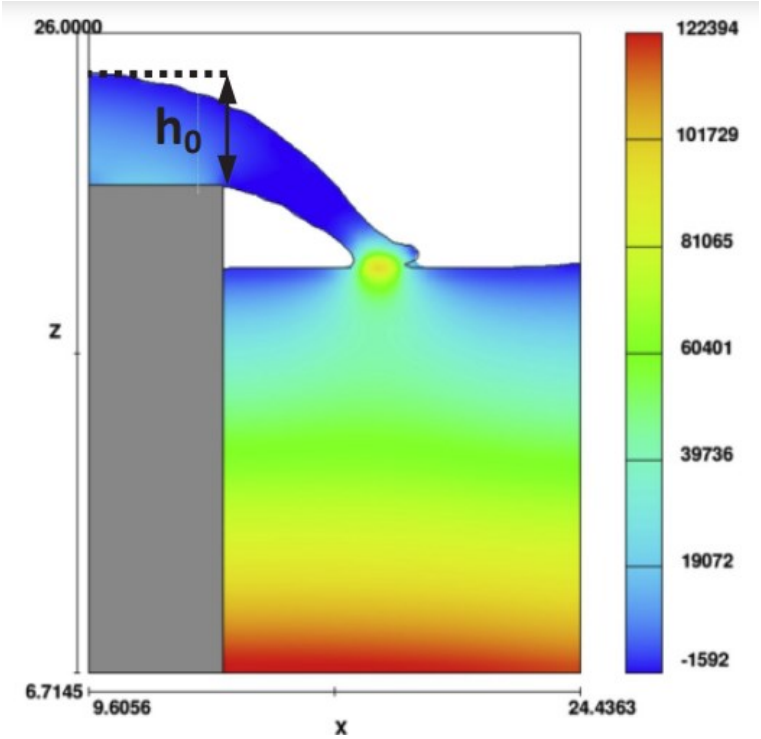

Figure 19. Definition of h0.

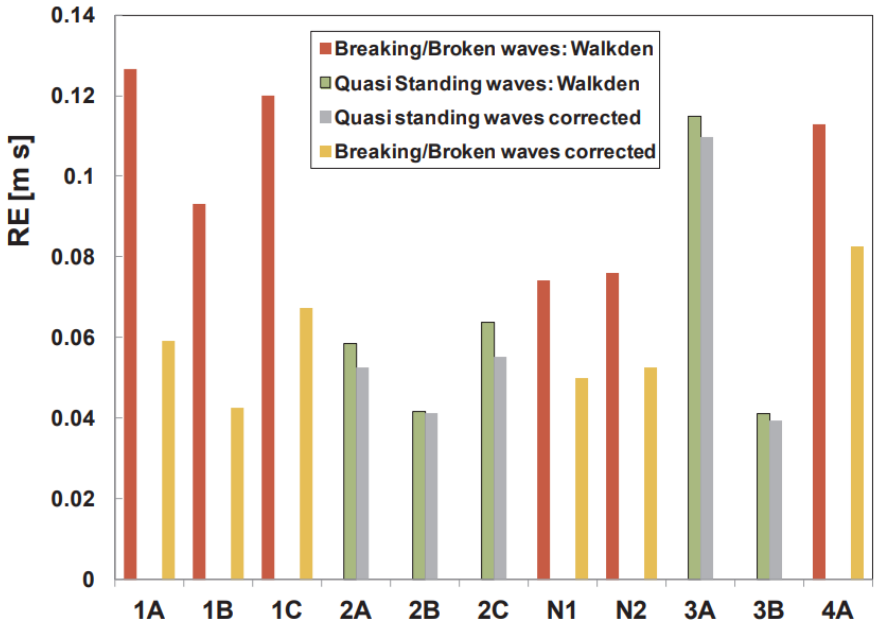

Figure 20. Effect of Eq. (15) on the Walkden et al. theory

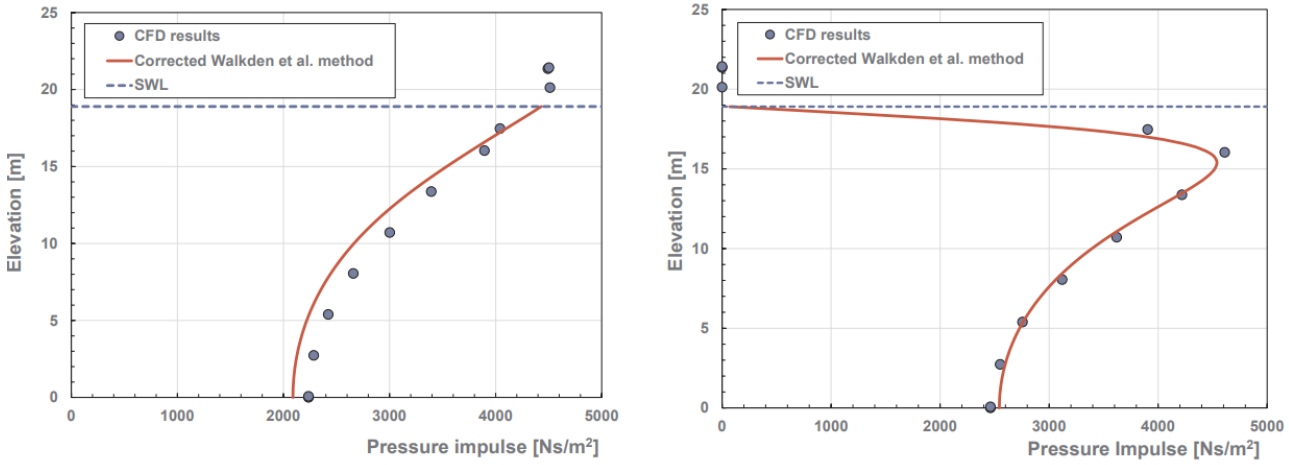

Figure 21. Effect of Eq. (15) on the events of Fig. 20

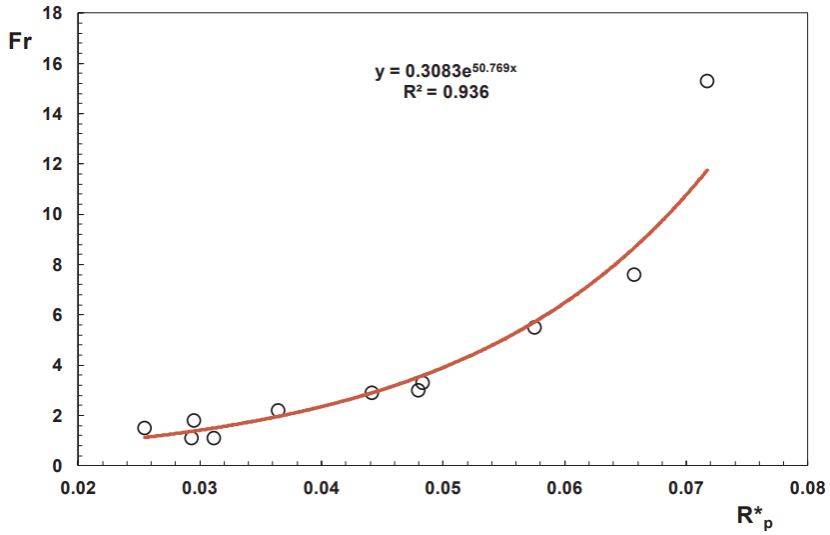

Figure 22. Optimal Froude number as function of the crest freeboard.

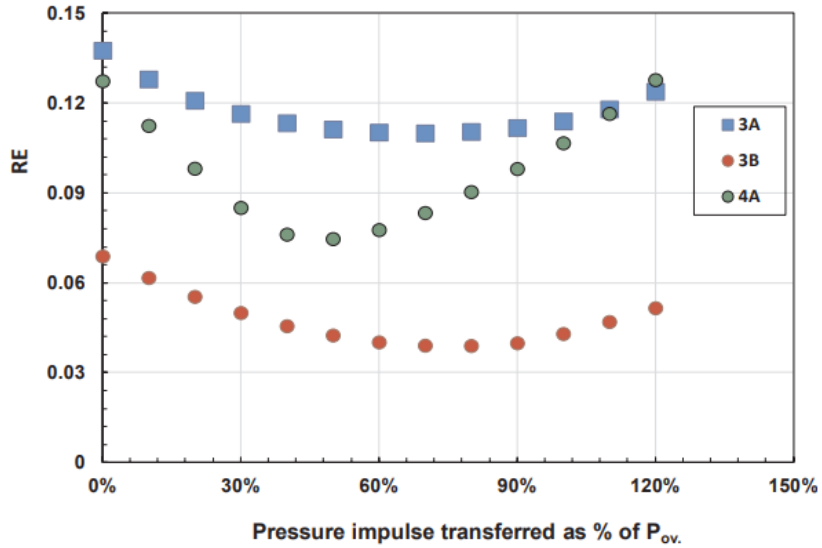

Figure 23. Effect of the pressure impulse transferred by the air pocket on the performance of the Walkden et al. (2001) method.

4. Summary and conclusions

With the aid of the Computational Fluid Dynamics technique, which is now growing popular as a research tool in the field of coastal and ocean engineering (e.g. Jun and Meng, 2011 Kamath, 2015; Antonini et al., 2016, 2017; Miquel et al., 2018), impulsive events generated by wave overtopping have been studied. The latter are termed “plume impacts” and consist of impact pressures exerted onto the inner face of the breakwaters, due to the huge inertia transferred in the protected area by the overtopping jet. Despite extreme interest to engineers, the “plume impact” has been almost ignored so far; the only research is the pioneering work of Walkden et al. (2001), who highlighted the existence of such phenomenon based on 3 individual wave events in a small scale laboratory. In view of this lack of knowledge, this paper has willed to provide more systematic information, with a special focus on the macrofeatures of the impact, the magnitude of loadings, the distribution of pressures and, more in general, the predictability of the phenomenon. In the frame of a probabilistic approach, formulae for mean and variance of the force peak, force rise time and pressure peak have been given, to serve as reference for future research works. In this respect, one of the most interesting outcomings is the correlation between large plume impacts and intense impact loadings on the front face of the caisson. This experimental finding is physically explained by the fact that when waves break in front of the structure, high flow velocities develop, which increase the momentum of the overtopping jet. This process has been incorporated in the theoretical prediction method proposed by Walkden et al. by including the kinetic height of the overtopping current in the boundary problem that permits estimating the pressure impulse at the wall. The correction above mentioned proved to significantly increase the prediction power of the Walkden et al. method in case of breaking and broken waves, whereas for standing waves, only small improvements have been obtained. Finally, the distribution of pressures resulted significantly affected by the presence of air, which has been observed to rule the location of either the pressure barycentre or maximum of pressure distribution.

Acknowledgment
The authors gratefully acknowledge Eng. Fabio Maresca for his assistance in data analysis and as well as the two anonymous reviewers for their precious suggestions.

REFERENCES

Antonini, A., Lamberti, A., Archetti, R., Miquel, A.M., 2016. CFD investigations of OXYFLUX device, an innovative wave pump technology for artificial downwelling of surface water. Appl. Ocean Res. 6, 16–31.
Antonini, A., Archetti, R., Lamberti, A., 2017. Wave simulation for the design of an in novative quay wall: the case of Vlorë Harbour. Nat. Hazards Earth Syst. Sci. 17 (1), 127–142. https://doi.org/10.5194/nhess-17-127-2017. ISSN: 15618633.
Buccino, M., Vicinanza, D., Dalerno, D., Banfi, D., Calabrese, M., 2015. Nature and magnitude of wave loadings at sea-wave slotcone generators. Ocean Eng. 95, 34–58.
Buccino, M., Dentale, F., Salerno, D., Contestabile, P., Calabrese, M., 2016. The Use of CFD in the Analysis of Wave Loadings Acting on Seawave Slot-cone Generators. (Sustainability, MDPI).
Buccino, M., Daliri, M., Dentale, F., Calabrese, M., 2019. CFD Experiment on a Low Crested Sloping Top Breakwater. Part 1: nature of Loadings and Global Stability. Submitted to Ocean Engineering.
Bullock, G.N., Hewson, P.J., Crawford, A.R., Bird, P.A.D., 2000. Field and laboratory measurements on vertical breakwaters. Coastal Structures 99 editor I.J.Losada, Balkema, Rotterdam, 2: 613-622.
Bullock, G.N., Crawford, A.R., Hewson, P.J., Walkden, M.J.A., Bird, P.A.D., 2001. The influence of air and scale on wave impact pressures. Coast Eng. 42, 291–312.
Calabrese, M., Allsop, N.W.H., Buccino, M., 2000. Effect of random multidirectional wave fields on wave loads on vertical and composite breakwaters. In: Proceedings of the 27th International Conference on Coastal Engineering, vol. 2. pp. 1710–1723 Sydney, Australia, 16–21 July 2000.

Cooker, M.J., Peregrine, D.H., 1995. Pressure-impulse theory for liquid impact problems. J. Fluid Mech. 297, 193–214.
Cuomo, G., Allsop, W., Takahashi, S., 2010. Scaling wave impact pressures on vertical walls. Coast. Eng. 57, 604–609.
Gaeta, M.G., Lamberti, A., 2015. The role of air modeling on the numerical investigation of coastal dynamics and wave-structure interactions (2015). Comput. Fluids 111, 114–126.
Hseih, D.Y., Plesset, M.S., 1961. Theory of rectified diffusion of mass into gas bubbles. J. Acoust. Soc. Am. 33 (2).
Jun, J., Meng, B., 2011. Computation of wave loads on the superstructures of coastal highway bridges. Coast Eng. 38 (2011), 2185–2200.
Kamath, A., 2015. CFD Based Investigation of Wave-structure Interaction and Hydrodynamics of an Oscillating Water Column Device.
Kirkgoz, M.S., 1991. Impact pressure of breaking waves on vertical and sloping walls. Ocean Eng. 18 (Elsevier).
Kortenhaus, A., Oumeraci, H., 1999. Scale effects in modeling wave impact loading of coastal structures. In: Proc. HYDROLAB-workshop on Experimental Research and Synergy Effects with Mathematical Models Forschungszentrum Kuste, pp. 285–294 Hannover.
Miquel, A.M., Kamath, A., Chella, M.A., Archetti, R., Bihs, H., 2018. Analysis of different methods for wave generation and absorption in a CFD-based numerical wave tank. J. Mar. Sci. Eng. 6 (2) 73.
Owen, M.W., 1980. Design of Seawalls Allowing for Wave Overtopping. Rep. EX 924b. Hydraulics Research Station, Wallingford, England.
Peregrine, D.H., 2003. Water-wave impact on walls. Annu. Rev. Fluid Mech. 35, 23–44.
Vicinanza, D., 1997. Pressioni e forze di impatto di onde frangenti su dighe a paramento verticale e composite (In Italian). Ph.D. thesis). .
Vicinanza, D., Dentale, F., Salerno, D., Buccino, M., 2015. Structural response of seawave slot-cone generator (SSG) from random wave CFD simulations. In: Proceedings of the International Offshore and Polar Engineering Conference (ISOPE 2015). 2015- January, pp. 985–991.
Walkden, M.J., Wood, D.J., Bruce, T., Peregrine, D.H., 2001. Impulsive seaward loads induced by wave overtopping on caisson breakwaters. Coast Eng. 42, 257–276 2001.
Wood, D.J., Peregrine, D.H., Bruce, T., 2000. Study of wave impact against a wall with pressureimpulse theory. Part 1: trapped air. J. Waterw. Port Coast. Ocean Eng. ASCE 126, 182–190.